Carcinogenesis vol.25 no.6 pp.909–921, 2004
DOI: 10.1093/carcin/bgh075

RasGTPase-activating protein is a target of caspases in spontaneous apoptosis of lung carcinoma cells and in response to etoposide

Babett Bartling[1], Jiang-Yan Yang[2], David Michod[2], Christian Widmann[2], Rolf Lewensohn[3] and Boris Zhivotovsky[1,4]

[1]Institute of Environmental Medicine, Division of Toxicology, Karolinska Institutet, Stockholm, Sweden, [2]Institut de Biologie Cellulaire et de Morphologie, Université de Lausanne, Lausanne, Switzerland and [3]Institute of Oncology and Pathology, Unit of Medical Radiobiology, Cancer Centre Karolinska R8:00, Karolinska Institutet, Stockholm, Sweden

[4]To whom correspondence should be addressed.
Email: boris.zhivotovsky@imm.ki.se

p120 RasGTPase-activating protein (RasGAP), the main regulator of Ras GTPase family members, is cleaved at low caspase activity into an N-terminal fragment that triggers potent anti-apoptotic signals via activation of the Ras/PI-3 kinase/Akt pathway. When caspase activity is increased, RasGAP fragment N is further processed into two fragments that effectively potentiate apoptosis. Expression of RasGAP protein and its cleavage was assessed in human lung cancer cells with different histology and responsiveness to anticancer drug-induced apoptosis. Here we show that therapy-sensitive small lung carcinoma cell (SCLC) lines have lower RasGAP expression levels and higher spontaneous cleavage with formation of fragment N compared to therapy-resistant non-small cell lung carcinoma cell (NSCLC) lines. The first RasGAP cleavage event strongly correlated with the increased level of spontaneous apoptosis in SCLC. However, generation of protective RasGAP fragment N also related to the potency of SCLC to develop secondary therapy-resistance. In response to etoposide (ET), RasGAP fragment N was further cleaved in direct dependence on caspase-3 activity, which was more pronounced in NSCLC cells. Caspase inhibition, while effectively preventing the second cleavage of RasGAP, barely affected the first cleavage of RasGAP into fragment N that was always detectable in NSCLC and SCLC cells. These findings suggest that different levels of RasGAP and fragment N might play a significant role in the biology and different clinical course of both subtypes of lung neoplasms. Furthermore, constitutive formation of RasGAP fragment N can potentially contribute to primary resistance of NSCLC to anticancer therapy by ET but also to secondary therapy-resistance in SCLC.

Introduction

Lung carcinoma represents the leading cause of malignancy-related mortality (1). Therefore, much attention has been given to identify targets in the treatment of human lung cancer. One of the most frequently used targets of drug classes is the nuclear enzyme DNA topoisomerase II (2). Topoisomerases are involved in several cellular events during the cell cycle such as DNA replication, transcription, recombination and chromatid segregation. Among the topoisomerase II-affecting agents currently in clinical use is etoposide (ET). ET stabilizes topoisomerase II-associated double-strand DNA breaks by inhibiting the enzyme ability to ligate cleaved nucleic acid molecules. However, ET does not only inhibit the cell cycle but also affects other cellular functions. The ET targets are referred to as pre-targets when they correspond to plasma membrane and cytosolic components and to post-targets when they participate in gene regulation. In this regard, cellular perturbation caused by ET is also realized via initiation of apoptotic cell death (3). Proteolytic activation of a cascade of caspases, a family of cysteine proteases that cleave their substrates after aspartate residues, is considered as the central element of the apoptotic machinery (4). The cascade is started by auto-activation of initiator caspases, triggered either by ligand binding to death domain receptors (extrinsic pathway) or by cytosolic translocation of apoptogenic factors from mitochondria (intrinsic pathway). While the initiator caspase pro-caspase-8 mediates the receptor-induced apoptosis, release of cytochrome *c* from mitochondria leads to the activation of pro-caspase-9 in an apoptosome complex thereby mediating the mitochondrial-dependent pathway (5). The subsequent proteolytic activation of executioner caspases, like pro-caspase-3, -6 and -7, results in the processing of a large variety of cellular substrates. Those substrates are activated, deactivated or acquire new functions once cleaved by caspases and contribute to the characteristic morphological and biochemical changes that occur during apoptosis (6).

However, caspase activation does not always result in the proteolysis of cellular determinants participating in cell death. Recently, it has been shown that p120 RasGTPase-activating protein (RasGAP), the main down-regulator of Ras GTPase family members (7), is a substrate for caspases that differentially regulates apoptosis as caspase activity increases in cells (8). Depending on the extent of its processing by caspases, RasGAP fragments stimulate survival signals at low levels of caspase activity but contribute to the execution phase of apoptosis when caspase activity is increased. The first cleavage of RasGAP occurs at position 455 at very low caspase activity (8). The resulting N-terminal fragment triggers potent anti-apoptotic mechanisms while the C-terminal fragment, containing the GTPase-binding function, leads to cell death in Ras-independent manner (8). However, the anti-apoptotic properties of fragment N are dominant over the pro-apoptotic abilities of fragment C (8). The N-terminal fragment consists mainly of Src homology (SH) domains, which have an important dynamic role in recruiting GAPs to specific signalling complexes. Detailed investigation showed that RasGAP fragment N is a potent inhibitor of apoptosis down-stream of

Abbreviations: ET, etoposide; GAP, RasGTPase-activating protein; IKKα, IkappaB kinase α; NFκB, nuclear factor κB; NSCLC, non-small cell lung carcinoma; PARP, poly(ADP-ribose) polymerase; PBS, phosphate-buffered saline; PI-3 kinase, phosphatidylinositol 3-kinase; SCLC, small cell lung carcinoma; ST, staurosporine; TdT, terminal deoxynucleotidyltransferase.

caspase activation as shown for caspase-9 (8). Although fragment N does not contain the GAP domain, it effectively protects cells by initiating the chain of protein reactions involved in the Ras-mediated pathway. The homology domain SH3, which is flanked by two SH2 domains, has been suggested to be involved in this process (9). Subsequent activation of the phosphatidylinositol (PI)-3 kinase results in the phosphorylation of target proteins that contain pleckstrin homology domains for binding to the inner plasma membrane. In RasGAP fragment N signalling, the serine/threonine kinase Akt (also known as protein kinase B) has been shown to be an effector of the PI-3 kinase pathway (10) via PDK1 (3-phosphoinositide-dependent kinase)-mediated phosphorylation (11). The PI-3 kinase-induced stimulation of Akt can contribute to cell survival through a number of mechanisms. This includes the inhibition of Bad activity (12) but also the suppression of Bax translocation to mitochondria (13), blocking of procaspase-9 activation (14) and stimulation of the transcription factor NFκB activity via IkappaB kinase α (IKKα) (15). However, NFκB plays no role in the anti-apoptotic function of fragment N (10). At higher levels of caspase activity, the protective effect of RasGAP fragment N is abolished when fragment N is cleaved at position 157. This second cleavage event causes the formation of two N-terminal RasGAP fragments, named N1 and N2, which can effectively potentiate apoptotic cell death (8).

The aim of the present study was to investigate the expression and cleavage pattern of RasGAP in a panel of lung cancer cell lines with different histology and sensitivity to anticancer treatment. Human lung carcinomas are broadly classified into non-small cell lung carcinomas (NSCLC) and small cell lung carcinomas (SCLC). This simplified grouping is based on the histology, biology and clinical behaviour of the tumours and their treatment options (16). Both subtypes differ in their initial responsiveness to chemotherapeutic agents including ET (17). While chemotherapy provides rather poor response rates in NSCLC patients with rare complete remissions, SCLC belong to the most drug-sensitive tumours. SCLC accounts for ~20–25% of all human lung cancers and, despite primary chemo- and radiosensitivity, SCLC bears the poorest prognosis of all lung cancer histologies due to fast tumour expansion, early metastasis and high incidence of relapse along with the subsequent development of therapy resistance (18). Therefore, the resistance to treatment represents the major problem in the therapy of NSCLC and SCLC as well. The poor responsiveness to topoisomerase II inhibitors might link to increased expression of topoisomerase II, lowered drug accumulation due to expression of membrane 'pump' proteins, altered cytotoxic signalling through stress-activated protein kinases and alterations in cell cycle proteins (19). Previously, it has been shown that the different susceptibility of SCLC and NSCLC to undergo apoptosis is related to the reduced drug response of malignant lung neoplasm (20). While SCLC cells undergo cell death in caspase-dependent and -independent manner, the caspase-mediated pathway of apoptosis is inefficient in NSCLC mainly because of a defective translocation of active caspase-3 into the nucleus (21). While the reduced nuclear localization of caspase-3 represents a key regulator of cell death influencing the responsiveness to chemotherapeutic agents in NSCLC, mechanisms involved in the acquired chemoresistance in SCLC are not yet fully understood.

The PI-3 kinase/Akt pathway has been found to play a significant role in the survival of experimental cancer cell lines including NSCLC and SCLC (22,23). Furthermore, altered expression of RasGAP is involved in tumorigenesis as well (24) that might consequently lead to an impaired controlling of p21 Ras signalling and other down-stream signalling pathways (7). Based on these observations and that generation of the N-terminal RasGAP fragment participates in survival mechanisms via PI-3 kinase/Akt, we were interested in analysing the level of RasGAP and its N-terminal cleavage products in NSCLC and SCLC upon treatment of lung cancer cell lines with ET in relation to caspase activity and extent of apoptosis.

Material and methods

Antibodies and reagents

An antisera against the N-terminal moiety of RasGAP was produced in rabbits injected with a fusion protein consisting of a stretch of 6 histidine linked to amino acids 158–455 of RasGAP. This antigen was produced in BL21 (DE3) pLysS bacteria (Novagen, Madison, MI) and purified by using a Ni–NTA affinity column (Qiagen AG, Basel, Switzerland), as follows. Bacteria corresponding to a 1 l culture were lysed and sonicated in 40 ml of lysis buffer (50 mM HEPES, 500 mM NaCl, 10% Triton X-100, 20 mM Mg–acetate, 0.5% β-mercaptoethanol, proteases inhibitor cocktail from Roche Diagnostics (Mannheim, Germany), 2 mg/ml lysozyme, ~25 μg/ml DNase I). The bacterial lysate was incubated for 45 min at 4°C with 1 ml of Ni–NTA beads, washed three times with 1 ml of lysis buffer containing 25 mM imidazole. The antigen was then eluted with 600 μl of lysis buffer containing 200 mM imidazole. The eluate was dialysed two times against 5 l phosphate-buffered saline (PBS) to remove imidazole and kept at −80°C until further use. Antibodies specific for RasGAP were further purified as follows. Three millilitres of the antisera diluted 10 times in 10 mM Tris–HCl (pH 7.5) were loaded three times on a column containing 300 μl of Affigel 15 beads (Bio-Rad Laboratories, Hercules, CA) on which 1.5 mg of the antigen was coupled covalently. The beads were washed with 6 ml 500 mM NaCl, 10 mM Tris–HCl (pH 7.5) and 6 ml 10 mM Tris–HCl (pH 7.5). The antibody against RasGAP was eluted by using 3 ml of 100 mM glycine (pH 2.5) and recovered in 300 μl of 1 M Tris–HCl (pH 8.0). The antibody was stored at −20°C until use. The antibody directed to the C-terminal moiety of RasGAP was from Alexis (ALX-210-781; Lausanne, Switzerland). Rabbit polyclonal antibodies against caspase-3, -8 and -9, or mouse monoclonal antibodies against cytochrome *c* and poly(ADP-ribose) polymerase (PARP) (all are from BD Pharmingen, San Diego, CA) were applied in PBS-T buffer (10 mM Na_2HPO_4, 140 mM NaCl, 0.15% Tween 20; pH 7.35). Equal protein loading was controlled by using the polyclonal antibody against glyceraldehydes-3-phosphate dehydrogenase (GAPDH; Trevigen, Gaithersburg, MD). Bound antibodies were detected by horseradish peroxidase-conjugated goat anti-rabbit IgG or goat anti-mouse IgG antibodies (Pierce, Rockford, IL), respectively, which were diluted in PBS-T supplemented with 2% non-fat dry milk.

Lung cancer cells were treated with ET (Vepesid®, VP16; Bristol-Myers Squibb, Bromma, Sweden), staurosporine (ST) (Roche Diagnostics) or the agonistic αFas monoclonal antibody (SY-001; Medical & Biological Laboratories, Nagoya, Japan) to induce cell death. The cell permeable peptide zVAD-FMK was applied as pan-caspase irreversible inhibitor, zDEVD-FMK for inhibiting caspase-3/-7 and zIETD-FMK for caspase-8 activities, respectively (all are from Enzyme Systems Products, Livermore, CA). The fluorogenic substrates Ac-DEVD-AMC and Ac-LEHD-AMC (Peptide Institute Inc., Osaka, Japan) were used for the determination of proteolytic caspase activities.

Cell lines, culture conditions and treatment

Human cell lines that were analysed correspond to NSCLC (A549, H23, H125, H157, H661, U1752 and U1810) or to SCLC (H69, H82, H592, U1285, U1690 and U1285dox, a doxorubicin-resistant variant of U1285). All cell lines of H denotation have the prefix National Cancer Institute (NCI). Additionally, HeLa cells (human cervix carcinoma) and Jurkat cells (human T cell leukemia) were investigated as a non-lung cancer control. Lung cancer cell lines of U denotation are characterized earlier (25), cell lines of A or H denotation, HeLa and Jurkat (TIB 152) are purchased from the ATCC cell bank (Manassas, VA). Cells were cultured in RPMI 1640 medium supplemented with 7.5% heat-inactivated foetal bovine serum, 2 mM L-glutamine, 100 U/ml penicillin and 100 μg/ml streptomycin (Invitrogen Life Technology, Täby, Sweden) in 5% CO_2 atmosphere at 37°C.

Twenty-four hours after seeding in culture dishes with fresh medium, cells were treated by adding ET (2.5–10 μM, 48 h), ST (1 μM, 2–6 h) or the

agonistic αFas monoclonal antibody (200 ng/ml, 24 h). Mock-treated cells of long-term experiments were seeded initially at less density to keep control cells at levels allowing exponential growth. The caspase inhibitory peptides zVAD-FMK, zDEVD-FMK and zIETD-FMK were used at 20 μM final concentration and added 1 h prior to treatment.

Cell death analysis

Apoptosis was analysed by investigation of nuclear alterations. An aliquot of the cells was re-suspended in PBS, spread on slides and allowed to air-dry. After fixation with acetone and staining with 1 μg/ml Hoechst 33342 in PBS (Molecular Probes Europe, Leiden, The Netherlands), 400 cells were assessed in each sample and scored as percentage of cells with fragmented and condensed nuclear morphology. *In situ* nuclear DNA fragmentation was determined by terminal deoxynucleotidyltransferase (TdT)-mediated dUTP nick end-labelling (TUNEL). Cells were prepared on slides, fixed with 3.7% paraformaldehyde (pH 7.4) and permeabilized with 0.1% Triton X-100 in PBS. After blocking with 3% bovine serum albumin in PBS and pre-incubation in TdT reaction buffer (pH 6.6), TUNEL reaction was carried out in a humidified chamber with 5 μM Fluorescein-12-dUTP, 50 μM dATP, 2.5 mM $CoCl_2$ and 25 U TdT (Roche Diagnostics) in TdT buffer at 37°C for 1 h. Thereafter, slides were co-stained with Hoechst 33342 in PBS and mounted with 50% glycerol in PBS. Samples were examined with an Olympus BX60 fluorescence microscope (excitation wavelength 365 nm) and images collected using the Hamamatsu digital camera ORCA II.

$SubG_1$ DNA content was quantified by staining of DNA with propidium iodide (PI; Sigma, Deisenhofen, Germany) and subsequent flow cytometry. Briefly, PBS-rinsed cells were fixed with ice-cold 70% ethanol and incubated with PI solution (50 μg/ml PI, 5 mg RNase A, 0.1% Triton X-100, 0.1% sodium citrate, 0.1 mM Na_2EDTA in PBS; pH 7.2) for 1 h at 4°C. DNA content was measured using the FACScan flow cytometer equipped with Cell Quest software (Becton Dickinson, San José, CA). Additionally, amount of cells with loss of the plasma membrane integrity was counted in a haemacytometer after viability staining with 0.2% trypan blue in PBS. Another hallmark of cell death, the release of cytochrome *c* from mitochondria, has been quantified by immunoblot analysis of cytosolic protein preparations (see below).

In vitro caspase assay

Caspase activity was measured by cleavage of fluorogenic substrates specific for caspase-3-like proteases (Ac-DEVD-AMC) and caspase-9 (Ac-LEHD-AMC). Briefly, 2.5×10^5 cells were seeded initially. After treatment, cells were re-suspended in 30 μl PBS and 25 μl were transferred to a 96-well plate. The remaining cell aliquot was kept for protein determination using the BCA protein assay (Pierce, Rockford, IL). Enzyme reaction was performed at 37°C by adding 50 μl of either HEPES buffer (100 mM HEPES, 10% sucrose, 0.1% CHAPS, 5 mM DTT, 10^{-6}% NP-40; pH 7.25) for caspase-3/-7 or MES buffer (100 mM MES, 10% sucrose, 0.1% CHAPS, 5 mM DTT, 10^{-6}% NP-40; pH 6.5) for caspase-9 containing 30 μM of the respective peptide substrate. AMC liberation was monitored by a Fluoroscan II plate reader (Labsystems, Stockholm, Sweden) at 355 nm excitation and 460 nm emission, finally converted to pmol of AMC release per min and normalized per mg protein.

Protein extraction and immunoblot analysis

For preparation of cytosolic protein fraction, samples were incubated in isolation buffer (20 mM HEPES, 10 mM NaCl, 120 mM KCl, 1 mM KH_2PO_4, 1 mM $MgCl_2$, 250 mM sucrose, 2 mM Na_2ATP; pH 7.2) containing 10 μg digitonin per 1×10^6 cells and protease inhibitor cocktail (Roche Diagnostics). After 5 min of incubation at room temperature, lysates were cleared by centrifugation at 15 000 *g* for 10 min. In the case of total protein extraction, 1% Triton X-100 was added to the isolation buffer. Protein concentration was measured by the BCA protein assay (Pierce). All protein samples were mixed with 4× loading buffer (500 mM Tris–HCl, 40% glycerol, 8% SDS, 80 mM DTT, 4 mM Na_2EDTA, 0.2% bromophenol blue; pH 7.4), boiled for 2 min and separated using SDS–PAGE. Proteins of the analytic gel were blotted onto a nitrocellulose membrane in 10 mM CAPS buffer/20% methanol (pH 11.0) by the Bio-Rad wet blotting system (Bio-Rad Laboratories, Sundbyberg, Sweden). Thereafter, the membrane was blocked with 6% non-fat dry milk in PBS-T and incubated with the respective antibody. Primary antibodies were detected by horseradish peroxidase-conjugated secondary antibodies and subsequently visualized by the ECL^{plus} substrate solution (Amersham, Buckinghamshire, UK) according to manufacturer's instruction. The intensity of visualized signals was densitometrically analysed using the Aida evaluation software (Raytest, Straubenhardt, Germany).

Statistics

The significance of comparison of mean values was determined by the Student's *t* test. The one-way ANOVA procedure or the ANOVA analysis on Ranks for non-parametric groups was used for multiple comparisons. The correlation coefficient *r* of the linear regression analysis was tested using the two-sided test (SigmaStat software; Jandel, San Rafael, CA). All data reported are given as mean ± SEM with $P < 0.05$ as indicating a significant difference.

Results

RasGAP expression in human lung cancer cell lines

Immunoblot analyses of a panel of human lung cancer cell lines demonstrated that in basal conditions NSCLC cells show higher expression level of p120 RasGAP compared with SCLC cells (Figure 1A and B). These results are based partially on the fact that SCLC cell lines displayed increased processing of the full-length RasGAP protein into the N-terminal RasGAP fragment. As summarized in Table I, SCLC cells are characterized by an elevated level of spontaneous apoptosis as estimated by nuclear DNA fragmentation. While 9 ± 2% of apoptotic cells have been identified in SCLC cell lines, NSCLC cell lines showed nuclear features of apoptosis in <1% of cells ($P < 0.01$ versus SCLC). Subsequent linear regression analysis revealed a significant, positive correlation between the number of cells with spontaneous apoptosis and the relative cleavage of fragment N per RasGAP in human lung carcinomas (Figure 1C).

Cell death and caspase activation induced by ET in SCLC and NSCLC

Two human lung cancer cell lines with different levels of spontaneous apoptosis and initial formation of RasGAP fragment N were selected from the whole panel and investigated in detail: U1810 as an example for NSCLC and H82 for SCLC (Table I). Both cell lines were subjected to treatment with increasing concentrations of ET (2.5–10 μM) for 48 h. In addition the broad-spectrum protein kinase inhibitor ST (1 μM, 2–6 h) and the agonistic αFas antibody (200 ng/ml, 24 h) have been used to induce cell death (see below).

Figure 2 demonstrates that treatment of U1810 and H82 cells with ET resulted in a G_2/M phase cell cycle arrest with a strong tendency of U1810 cells to accumulate already in the S phase at higher concentrations (≥5 μM) of ET. The characterization of cell death triggered by ET and its influence by simultaneous inhibition of caspases using the broad-range inhibitory peptide zVAD-FMK (20 μM) is summarized in Table II. Taken together, these investigations revealed that loss of the plasma membrane integrity is a main feature of NSCLC U1810 cells undergoing ET-induced death, while the presence of apoptotic nuclei and $subG_1$ DNA fragmentation are less prominent. However, a certain amount of U1810 was also characterized by typical apoptotic changes such as nuclear condensation, formation of membrane blebbing and cell shrinkage without trypan blue uptake (Figure 2B). The inhibition of caspases by zVAD-FMK did not prevent ET-induced apoptosis in U1810 cells. Rather it slightly shifted U1810 cells towards features of necrosis as shown by an increased leakage of the plasma membrane (Table II). In contrast to U1810, SCLC H82 cells underwent a type of cell death more typical for apoptosis, which could be diminished following caspase inhibition by zVAD-FMK (Table II, Figure 2B). In response to 5 μM ET, the amount of cells with apoptotic nuclear morphology and hypoploidy, as well as the number of trypan blue-positive cells

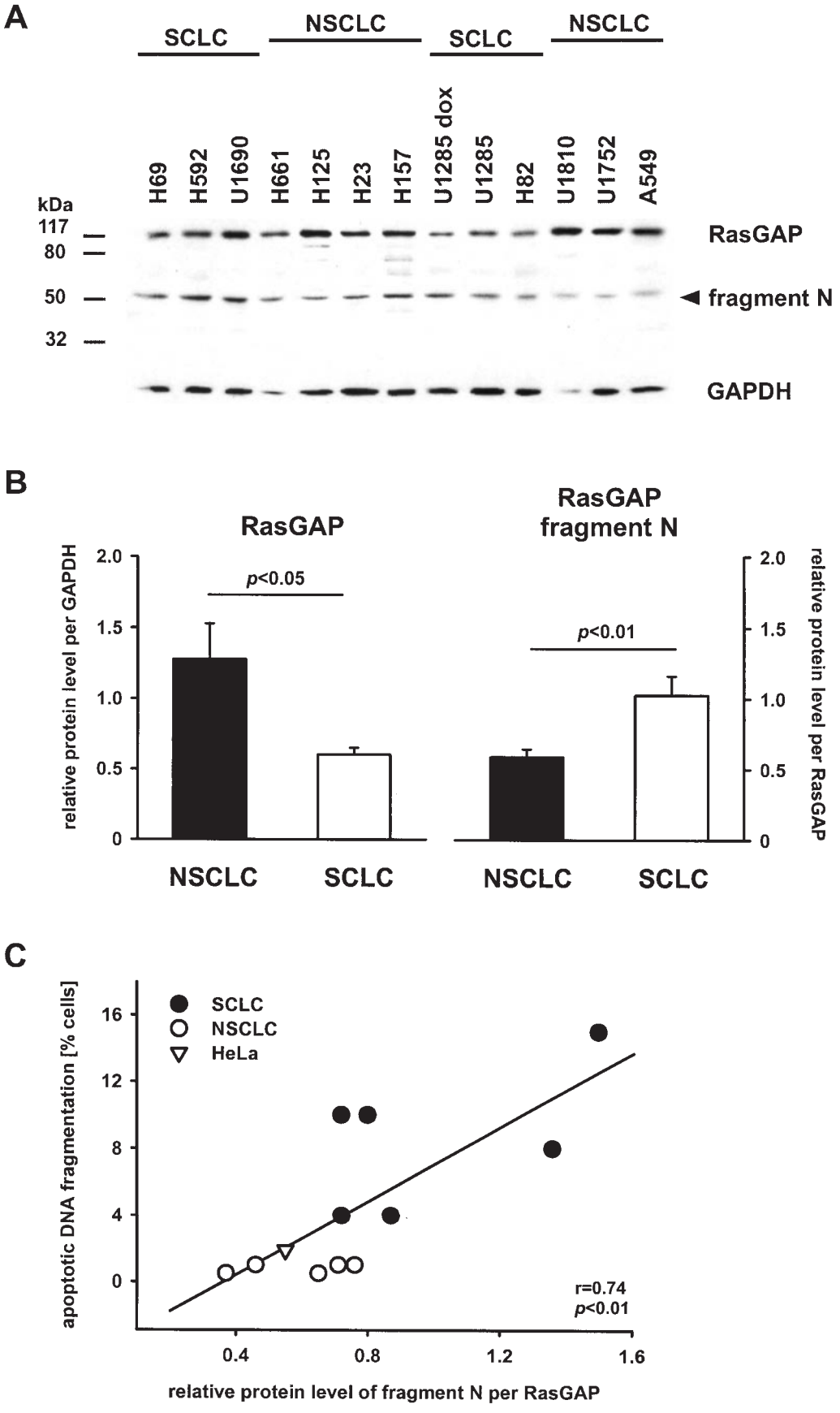

Fig. 1. (**A**) Detection and (**B**) quantification of RasGAP and RasGAP fragment N by immunoblotting in a panel of human lung cancer cell lines from NSCLC and SCLC. Given data are means ± SEM. (**C**) Linear regression analysis demonstrates a significant, positive correlation between relative cleavage of fragment N per RasGAP and spontaneous apoptotic DNA fragmentation in lung carcinoma cell lines ($n = 12$; r, linear regression coefficient).

Table I. Expression and cleavage of RasGAP in a panel of untreated human lung cancer cell lines

Lung cancer cell line	Histology	Mean RasGAP protein[a]	Mean ratio fragment N per RasGAP[b]	Spontaneous apoptosis (% cells)[c]
H69	SCLC	0.40	1.36	8
H592	SCLC	0.61	0.87	4
H82	SCLC	0.73	0.72	4
U1690	SCLC	0.71	0.72	10
U1285dox	SCLC	0.61	1.50	15
U1285	SCLC	0.56	0.99	10
A549	NSCLC, ACa	0.77	0.65	0.5
H23	NSCLC, ACa	0.87	0.71	1
H125	NSCLC, ACa	1.21	0.48	n.d.
H157	NSCLC, LCa	0.93	0.76	1
H661	NSCLC, LCa	2.12	0.69	n.d.
U1810	NSCLC, LCa	2.32	0.37	0.5
U1752	NSCLC, SSCa	0.71	0.46	1

ACa, adenocarcinoma; LCa, large cell carcinoma; SCCa, squamous cell carcinoma; n.d., not determined.
[a]Protein level for RasGAP is given as densitometrically determined value in relation to GAPDH.
[b]Ratio of RasGAP fragment N per full-length RasGAP. Samples from two different passages (passage 2 and 5) were analysed.
[c]Spontaneous apoptosis index is calculated from percentages of cells with subG$_1$ DNA fragmentation and TUNEL-positive nuclei.

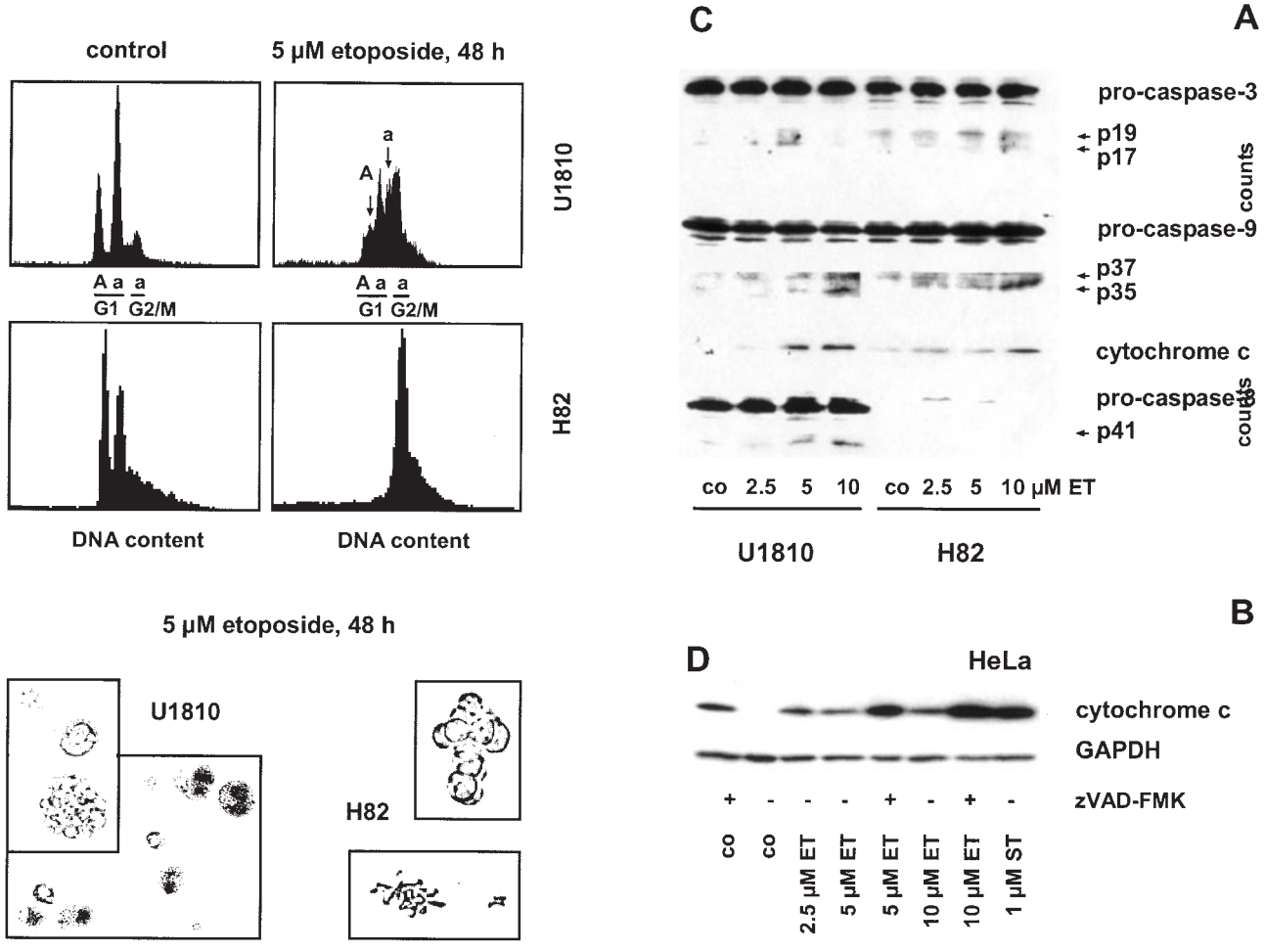

Fig. 2. (**A**) DNA staining of U1810 and H82 cells with propidium iodide and subsequent cell cycle analysis by cytometry after treatment with 5 µM ET (48 h). Arrows indicate aneuploid subpopulations (A,a) of U1810 cells in S phase. (**B**) Light microscopy of trypan blue-stained U1810 and H82 cells stimulated with ET as indicated. (**C**) The presence of pro-caspases and their proteolytically activated subunits (p) in cells stimulated with the indicated concentrations of ET for 48 h was analysed by western blot using total protein lysate (35 µg). The release of cytochrome *c* was analysed by western blot using cytosolic fraction (50 µg). (**D**) Detection of cytochrome *c* in cytosolic preparations of HeLa cells (50 µg) after ET treatment with and without zVAD-FMK (20 µM) in comparison with ST (4 h). GAPDH immunostaining indicates the same protein loading.

Table II. Characterization of cell death induced by ET and its influence by concomitant broad-range inhibition of caspases using zVAD-FMK

Cell line	ET treatment, 48 h	Apoptotic nuclei (%)[a]			$SubG_1$ DNA content (%)[b]	Cell viability loss (%)[c]	Cytosolic cytochrome *c* (%)[d]
		Mean fragmented	Mean condensed	Both features			
U1810	Control	0.6	1.8	2.3 ± 0.6	0.5 ± 0.2	4.9 ± 0.9	1.2 ± 0.3
	2.5 μM	3.1	5.3	8.5 ± 1.1	2.6 ± 0.8	13 ± 2.8	8.0 ± 1.6
	5.0 μM	3.3	8.9	11 ± 1.4	2.9 ± 0.5	16 ± 1.6	13 ± 2.1
	5.0 μM + zVAD-FMK	n.d.	n.d.	n.d.	2.7 ± 0.4	26 ± 5.5*	18 ± 3.0*
	10 μM	2.7	10	13 ± 2.3	3.9 ± 1.2	24 ± 2.7	21 ± 6.0
	10 μM + zVAD-FMK	2.8	10	13 ± 3.1	3.0 ± 0.4[e]	26 ± 4.2	22 ± 8.6
H82	Control	2.1	1.5	3.6 ± 0.6	2.2 ± 0.6	4.0 ± 0.6	8.6 ± 3.4
	2.5 μM	4.6	4.3	8.9 ± 1.7	4.6 ± 1.2	11 ± 1.4	14 ± 4.0
	5.0 μM	9.1	4.3	13 ± 0.9	6.2 ± 1.4	14 ± 1.1	21 ± 5.4
	5.0 μM + zVAD-FMK	n.d.	n.d.	n.d.	4.2 ± 1.0[e]	10 ± 2.6[e]	13 ± 4.9[e]
	10 μM	15	6.9	22 ± 3.3	7.5 ± 2.2	19 ± 2.1	21 ± 5.3
	10 μM + zVAD-FMK	5.2	6.1	11 ± 1.7[e]	4.7 ± 1.7[e]	13 ± 3.1[e]	19 ± 6.2
HeLa	Control	1.1	1.4	2.5 ± 0.6	1.8 ± 0.7	1.6 ± 0.4	3.7 ± 1.1
	2.5 μM	4.8	8.8	14 ± 4.2	2.3 ± 0.3	8.9 ± 2.0	12 ± 4.0
	5.0 μM	5.7	10	16 ± 2.9	2.4 ± 0.4	16 ± 2.7	15 ± 5.2
	5.0 μM + zVAD-FMK	n.d.	n.d.	n.d.	1.9 ± 0.2[e]	7.0 ± 1.0[e]	42 ± 5.8[e]
	10 μM	5.1	11	16 ± 2.0	2.4 ± 0.4	19 ± 2.8	22 ± 6.5
	10 μM + zVAD-FMK	3.1	7.3	10 ± 0.6[e]	1.8 ± 0.4[e]	16 ± 2.3[e]	46 ± 13[e]

n.d., not determined.
[a]Percentage of cells with apoptotic morphology as determined by Hoechst 33342 staining and microscopy.
[b]DNA hypoploidy measured by cytometry.
[c]Trypan blue uptake.
[d]Densitometry of immunoblot analysis for cytosolic level of cytochrome *c* per total amount, which was determined in presence of Triton X-100 and set to 100%. Data are given as mean ± SEM with $n \geq 5$, $n \geq 3$ (+zVAD-FMK, 20 μM).
[e]$P < 0.05$ versus ET treatment at the same concentration without zVAD-FMK.

and the extent of cytochrome *c* release, were clearly reduced in H82 cells treated with zVAD-FMK (Table II). At higher concentration of ET (10 μM), zVAD-FMK still mediated the inhibition of both the formation of the $subG_1$ peak and loss of cell viability, but the inhibition of cytochrome *c* release was nearly abolished (Table II).

Although U1810 cells displayed some necrotic features in response to ET treatment, these cells exhibited a high DEVD-proteolytic activity of caspase-3-like proteases compared with H82 cells (Figure 3). Caspase-9 was similarly activated in both lung carcinoma cell lines as measured by LEHD-AMC proteolysis (Figure 3). The corresponding cleavage of the pro-caspase-3 and pro-caspase-9 was also detected clearly along with the mitochondrial release of cytochrome *c* (Figure 2C). Furthermore, treatment of U1810 cells with ET resulted in the cleavage of pro-caspase-8, which is not expressed in most SCLC cell lines including H82 (Figure 2C).

It has been shown previously that the typical for apoptotic nuclear changes (e.g. DNA ladder formation) are less prominent in NSCLC cell lines because of the failure of caspase-3 to re-localize to the nucleus (26). Therefore, HeLa cells were analysed as a non-lung carcinoma cell line for comparison. In contrast to U1810 cells, HeLa cells display nuclear localization of active caspase-3 in response to ET despite a relative resistance towards the drug (27,28). In untreated conditions, the percentage of cells with apoptotic nuclei was comparable for HeLa and U1810 cells, but there were less HeLa cells taking up trypan blue compared with either U1810 or H82 cells (Table II). The amount of HeLa cells with spontaneous apoptosis correlated with the initial cleavage of RasGAP into fragment N (Figure 1C). Although the ET-induced death of HeLa cells was characterized by clear apoptotic morphology and plasma membrane leakage that could be reduced by zVAD-FMK (Table II), unchallenged HeLa cells released more mitochondrial cytochrome *c* in response to the caspase inhibitor (Figure 2D, compare the first two lanes), indicating that certain caspase-independent cell death pathways can be activated in these cells.

Spontaneous and ET-induced processing of RasGAP in lung cancer

Total protein preparations as well as cytosolic subfractions were used for the detection of RasGAP and its caspase-generated proteolytic fragments. To compare the cleavage of RasGAP with another caspase substrate, cleavage of PARP was also investigated.

The generation of the N-terminal RasGAP fragment already occurs in the presence of low caspase activities (8). However, *in vitro* cell culturing entails several factors of stress that might influence the initial cleavage of RasGAP into fragment N. Therefore, the level of spontaneously generated RasGAP fragment N has been observed throughout all experiments performed with U1810, H82 and HeLa cells. The range of the relative amount of fragment N per RasGAP was found to be comprised between 0.1 and 0.5 for U1810, between 0.25 and 1.0 for H82 and between 0.25 and 1.2 for HeLa cells. The mean ratios of fragment N per full-length RasGAP are summarized in Figure 4 in comparison with the spontaneous cell death determined for each cell line. This revealed a positive correlation between relative fragment N generation and the amount of apoptotic cells but an inverse tendency to the amount of cells with necrotic morphology.

In order to evaluate a relationship between the formation of anti-apoptotic RasGAP fragment N and the susceptibility of lung cancer cells to apoptosis, cells were treated with different concentrations of ET (2.5–10 μM) for 48 h. Protein separation (total cellular proteins or cytosolic preparations) revealed that, in contrast to full-length RasGAP and fragment N2, the

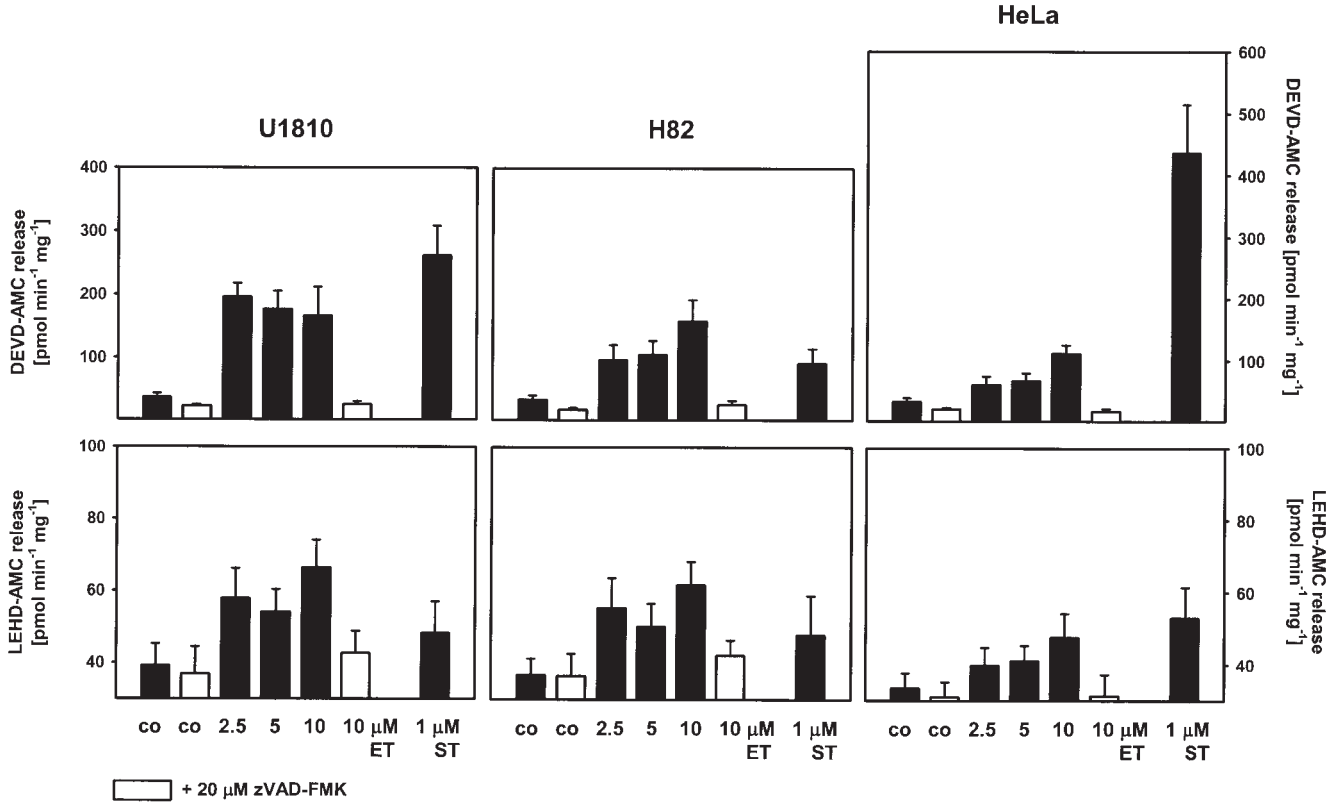

Fig. 3. Proteolytic caspase activity for caspase-3/-7 (above) and caspase-9 (below) after treatment of U1810, H82 and HeLa cells with increasing concentrations of ET (48 h) or with ST (4 h). White bars indicate concomitant incubation with the pan-caspase inhibitory peptide zVAD-FMK. All data are means ± SEM ($n \geq 5$).

RasGAP fragment N is not localized within the cytosol (Figure 5A). Confirming the results presented in Figure 1B, immunoblot analyses demonstrated that RasGAP is always expressed at the highest protein level in NSCLC U1810 cells and that the relative cleavage of RasGAP into fragment N in these cells is less induced than in H82 and HeLa cells. Generation of fragment N augmented in HeLa cells in response to increasing concentrations of ET (5–10 µM) (Figure 5A). This was not observed in both lung cancer cell lines.

As shown representatively on Figure 5A (left panel) ET induced the final cleavage of fragment N with formation of the pro-apoptotic RasGAP fragment N2 in NSCLC U1810 cells. This is in accordance with the elevated DEVD-proteolytic activity detected in U1810 cells, either directly in cell lysates (Figure 3) or indirectly by the assessment of PARP cleavage (Figure 5B). The caspase-mediated cleavage of RasGAP into fragment N2 was strongly reduced by broad-range inhibition of caspases using zVAD-FMK (Figure 5A, left panel). However, pan-caspase inhibitor zVAD-FMK did not influence the generation of RasGAP fragment N (Figure 5A, right panel).

Comparison of RasGAP cleavage mediated by treatment with ET, ST or αFas

There was similar proteolytic activity of caspase-3-like proteases induced in H82 and U1810 cells by a 48-h treatment with ET or a 4-h exposure to ST (Figure 3). In contrast, ST induced a much stronger caspase-3-like activity in HeLa cells compared with ET, consistent with the observation that these cells underwent massive apoptosis in response to ST (91 ± 1% of apoptotic nuclei; $n = 4$). ST is known to trigger cell death effectively in all lung carcinomas (26), and treatment with this compound caused appearance of 27 ± 2% of apoptotic nuclei in U1810 and 40 ± 2% in H82 cells. In accordance with differences in caspase activation, ST induced the cleavage of RasGAP into the N- and C-terminal fragments more efficiently than ET (Figures 5A and 7A). The agonistic αFas antibody induced even less RasGAP processing into fragment N2 than ET in U1810 cells (Figure 6). No generation of fragment N2 could be detected in H82 cells treated with the αFas antibody (Figure 6), as expected as these cells lack pro-caspase-8 (Figure 2). In contrast to both lung carcinoma cell lines, Fas activation readily caused the cleavage of RasGAP into fragment N2 in HeLa and in Jurkat cells. This cleavage event was decreased by inhibition of caspase-3/-7 with DEVD-FMK and totally prevented by inhibition of caspase-8 using IETD-FMK (Figure 6).

Analysis of total protein preparations and cytosolic subfractions revealed that RasGAP fragment N, in contrast to the full-length RasGAP protein, displayed a non-cytosolic location (Figures 5A and 7A and B). However, partial localization of fragment N in the cytosol fraction could be detected in certain conditions. Indeed, cytosolic detection of RasGAP fragment N has been observed after severe cell death induction by ST (Figure 7A) and after ET-induced cell death with the concomitant inhibition of caspases in U1810 and HeLa cells (Figure 7B). Since the cleavage into fragment N2 was clearly reduced by zVAD-FMK, a possible explanation for the cytosolic detection of fragment N could be that cell death occurs along with the degradation of intracellular organelles, including nuclear disintegration or swelling and rupture of mitochondria. Consistent with this possibility is our observation

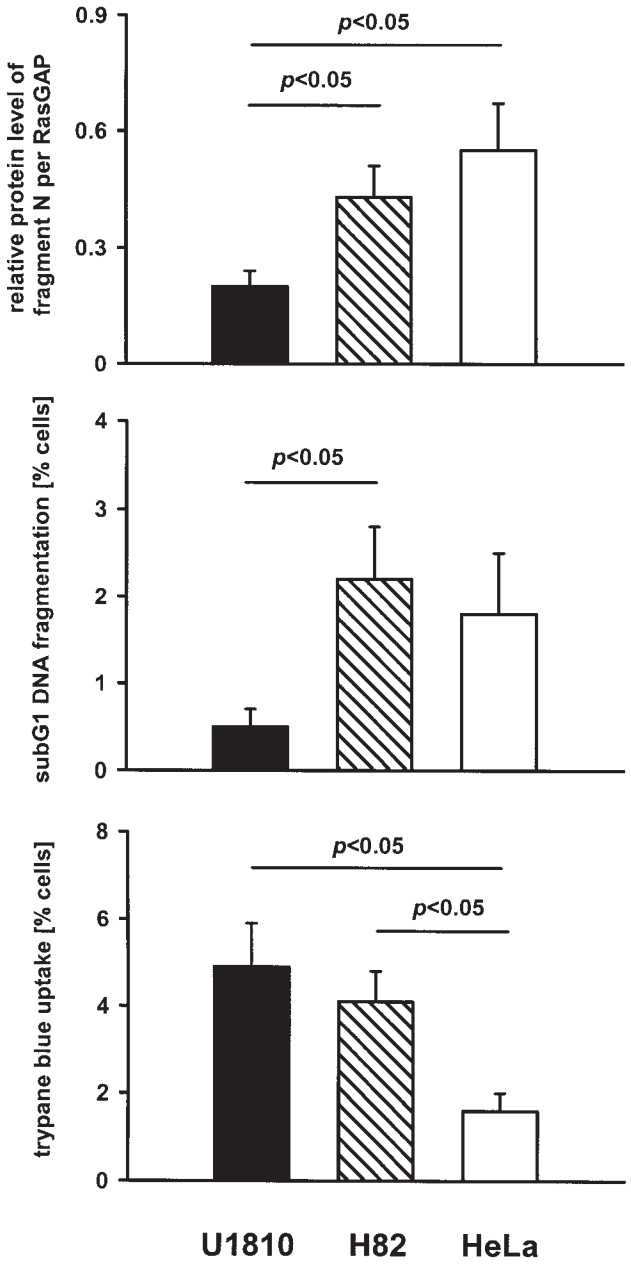

Fig. 4. Mean cleavage of full-length RasGAP into fragment N in U1810, H82 and HeLa cells. These results are derived from untreated controls of all experiments performed with ET, ST or αFas ($n = 8$). Multiple comparison by ANOVA procedure revealed a statistically significant difference among the groups as indicated ($P < 0.05$). Ratio of fragment N per RasGAP is shown in comparison with spontaneous cell death values for nuclear apoptosis (subG$_1$ DNA fragmentation) and cell viability staining (trypan blue uptake).

that PARP, which is excluded from the cytosolic subfraction in control conditions, translocates to this particular fraction upon stimulation with either ET in the presence of caspase inhibitor or in the presence of ST (Figure 7C).

Discussion

The family of p21 Ras proteins represents key components in the cellular signal transduction cascade leading to cell growth and differentiation. Function of p21 Ras family members has been linked to various processes that are important for cancer cell mutagenesis and metastasis (29). The regulation of Ras activity involves conversion of the inactive Ras-GDP to active Ras-GTP form in which RasGAPs contribute to the down-regulation of Ras by accelerating GTP hydrolysis of activated Ras. Five mammalian GAPs for Ras have been described including p120 RasGAP, the main GAP for this class of proteins (30). In this study, we have demonstrated that RasGAP is differentially expressed in SCLC and NSCLC cells. While NSCLC cell lines showed a strong expression of RasGAP protein, the mean RasGAP level was markedly decreased in SCLC cells. Previous studies already revealed a putative role for RasGAP in tumorigenesis. Although data for GAPs are rare in human lung neoplasm, the oncogenic potential of RasGAP due to mutations within the SH2 region are demonstrated in other malignancies, as well as nuclear re-localization and alterations in the gene expression (24,31). In this regard, an inverse correlation between the level of RasGAP and the invasive potential and malignant phenotype has been described (32,33). Based on the poor clinical prognosis of SCLC (18), our data additionally imply that low expression of RasGAP is associated with tumorigenesis and aggressive growth of SCLC. However, reduced availability of RasGAP could trigger two independent mechanisms. On one hand, it may be associated with the malignant behaviour of tumour cells, but, on the other hand, it may promote apoptotic cell death. In this context, Leblanc *et al*. revealed that RasGAP inhibition specifically induces apoptosis in tumour cells (34), an observation that could be related to the fact that SCLC display low levels of RasGAP and are characterized by relatively high level of spontaneous apoptosis (35). Furthermore, RasGAP deficiency also leads to neuronal cell death during embryonic development (36). In contrast to SCLC, RasGAP is well expressed in NSCLC suggesting that its main action in these cells is to act as a negative regulator of Ras activity. Nevertheless, one has to keep in mind that in contrast to SCLC, NSCLC often bear oncogenic mutations in the *ras* genes (29) that render the Ras proteins insensitive to RasGAP (37).

RasGAP is a dual function protein in the Ras signalling pathway because it also participates positively in cell signalling by mediating protein–protein interactions downstream of Ras- and Rho-dependent pathways (7,38). In the apoptotic process, the complex network of intracellular interactions via several protein domains in RasGAP is still intact despite its processing by caspases into several fragments. All generated forms of RasGAP have functional activity contributing to cell survival as well as to apoptosis (8). While the N-terminal cleavage product of RasGAP of the first cleavage event (fragment N) has anti-apoptotic property, the resulting C-terminal fragment as well as both N-terminal fragments (N1 and N2), generated due to the second cleavage event of fragment N, potentiate apoptosis. Analysis of a panel of human lung cancer cell lines revealed differential levels of RasGAP expression in NSCLC and SCLC, partially as a consequence of increased spontaneous RasGAP cleavage in SCLC cell lines compared with NSCLC cell lines. This primary processing of RasGAP into fragment N correlated with the higher level of spontaneous apoptosis in SCLC, an observation that might explain the initial RasGAP cleavage in the absence of apoptotic stimulus. Although RasGAP fragment N can protect cells via PI-3 kinase/Akt signalling (10), it may in some circumstances promote apoptosis in a Rho-dependent manner (34). Therefore and because of the parallel generation of the

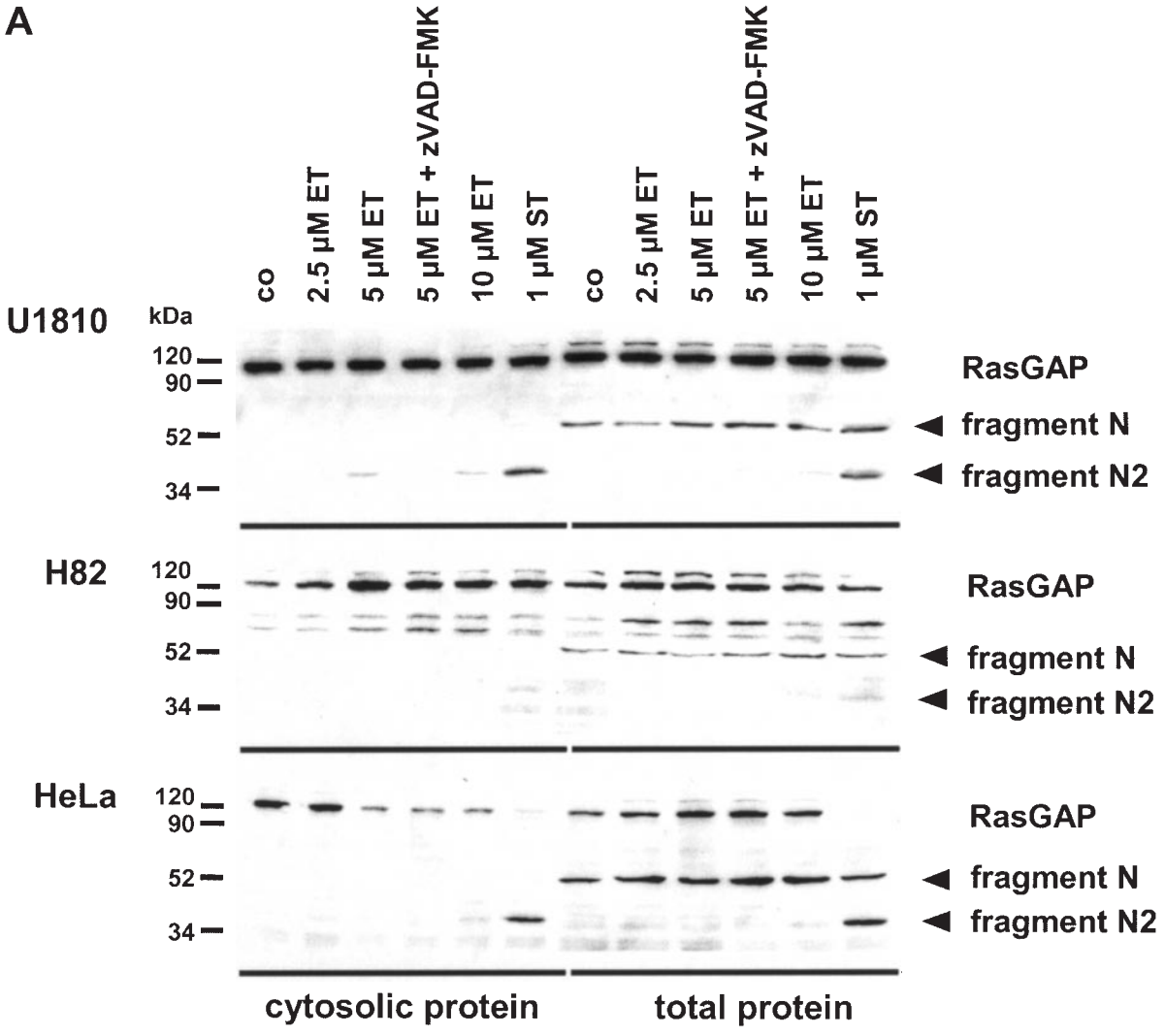

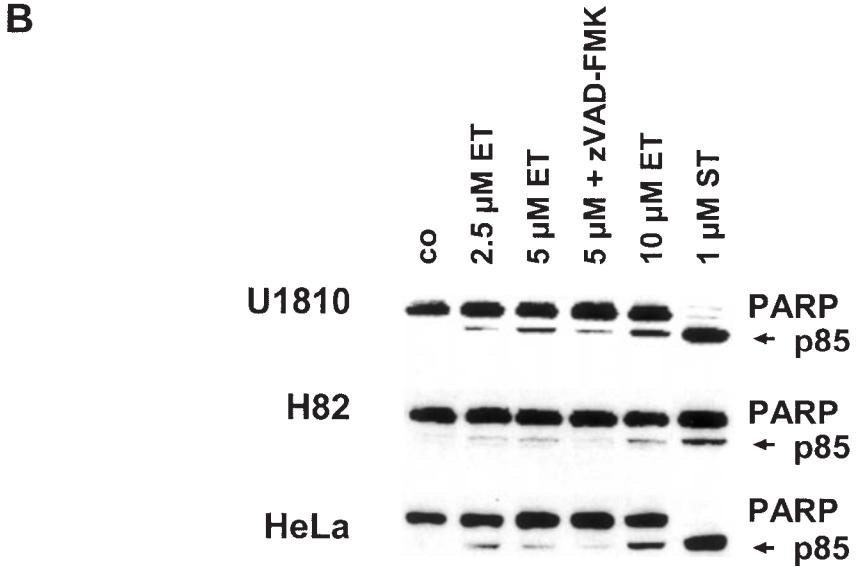

Fig. 5. (**A**) The presence of RasGAP and its N-terminal cleavage products was analysed by western blot in total protein lysate (50 µg) and cytosolic fraction (25 µg) from U1810, H82 and HeLa cells treated with different concentrations of ET (48 h) or with ST (4 h). zVAD-FMK (20 µM) was used to inhibit caspase activity. The cytosolic fraction contained RasGAP and fragment N2 but lacked fragment N. (**B**) The corresponding cleavage of PARP into fragment p85 was also analysed by western blot in total protein lysates.

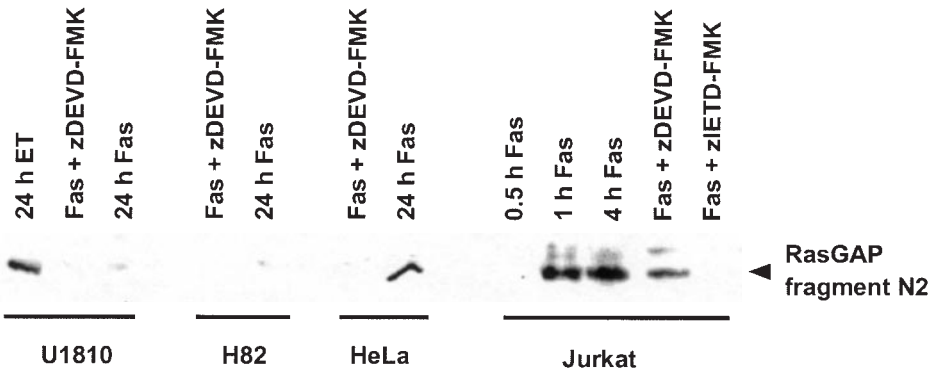

Fig. 6. Detection of RasGAP fragment N2 by western blot in U1810, H82 and HeLa cells treated for 24 h with the agonistic αFas antibody (Fas, 200 ng/ml), in U1810 cells subjected to a high-dose of ET (25 μM) for 24 h and in Jurkat cells stimulated with the αFas antibody for the indicated periods of time. Caspase inhibitors (zDEVD-FMK and zIETD-FMK at 20 μM) were added where indicated.

pro-apoptotic RasGAP fragment C, it is unclear if fragment N signalling is predominant in the molecular switch of SCLC cells. However, survival pathways initiated by RasGAP fragment N did overcome the opposite function of fragment C *in vitro* (8) and may participate in the constitutive activation of the Akt kinase observed in SCLC (39) and in the malignant phenotype of SCLC. The constitutive Akt stimulation has been shown to contribute to the transition of chemo- and radiosensitive SCLC cells to therapy-resistant tumours and transformation of classic (c-) SCLC to the insensitive variant (v-) SCLC (39). Although Akt is also activated in response to many growth factors (IGF-I, EGF, bFGF and others) and active Akt kinase has been shown in nearly 70% of patients with NSCLC as well (40), fragment N-mediated signalling represents an additional survival pathway in SCLC independent of the growth factor administration. Furthermore, we have revealed that RasGAP fragment N is not detectable in the cytosol whereas p120 RasGAP is. These findings raise the possibility that RasGAP proteins located at the plasma membrane and in other intracellular membranes are more accessible to proteolysis by caspases. Therefore, processing of RasGAP into fragment N would occur where RasGAP is actively regulating cell signalling. Alternatively, once formed, fragment N may immediately be targeted to non-cytosolic structures. There are peculiar cases, however, where fragment N is detected in the cytosolic fraction. For example, when caspases are inhibited in U1810 cells subjected to ET stimulation, a treatment that shifts the cells towards necrosis, fragment N and also PARP are detected in the cytosol. The increased generation of RasGAP fragment N might be one protective factor, especially in HeLa cells, that contributes to cell survival despite of intracellular necrotic changes.

The serine/threonine kinase Akt is phosphorylated and activated in response to apoptotic signals mediated by treatment of lung cancer cells with anticancer agents like ET (41). In our study we have demonstrated that generation of the Akt-stimulating RasGAP fragment N occurs after treatment of NSCLC and SCLC cells with ET as well. The formation of fragment N was relatively stable despite increasing concentrations of ET and always clearly detectable even with concomitant action of caspase-inhibitory peptides. This suggests a certain baseline proteolytic activity of caspases, which can be reduced but not completely abolished by action of peptide inhibitors. This observation furthermore indicates the high susceptibility of RasGAP for caspase proteolysis at its first cleavage site.

In contrast to the first cleavage of RasGAP into fragment N, the second cleavage of RasGAP fragment N into fragment N2 depends on the increased caspase activity in NSCLC and SCLC cell lines. While the activity of caspase-3-like proteases is high in NSCLC U1810 cells that readily generate RasGAP fragment N2, SCLC H82 cells did not display such a high proteolytic activity and were less able to produce fragment N2. Consistent with the notion that caspase-3 activity is required for the generation of fragment N2 is the observation that HeLa cells induce high level of caspase-3-like activity in response to ST and efficiently process RasGAP into fragment N2. In contrast to caspase-3-like proteases, a direct relationship between caspase-9 activity and terminal cleavage of RasGAP could not be drawn. The proteolytic rate of caspase-9 was low in comparison with caspase-3-like proteases in conditions where RasGAP was efficiently cleaved. One possible explanation for the differential activation of caspases could be that the continuous generation of RasGAP fragment N contributes, via PI-3 kinase/Akt stimulation, to phosphorylation and inactivation of caspase-9 (14).

In comparison with ET, the cell death-inducing effect of ST is more powerful although the anti-apoptotic RasGAP fragment N was generated as well. This might not only be based on the second cleavage event, transformation of fragment N into the pro-apoptotic fragment N2, but also on the fact that ST inhibits numerous kinases including PDK1 (42), which are required for the entire Akt function (11). Moreover, treatment with ST rapidly induces mitochondrial dysfunction in tumour cells (26) that might additionally overcome the protective effect of RasGAP fragment N.

Recent studies have shown that stimulation of the PI-3 kinase/Akt pathway precedes the onset of apoptosis and cleavage of PARP upon treatment with ET (41). The clear formation of RasGAP fragment N in all cell lines studied and its further generation in response to ET might be one component contributing to cell survival via PI-3 kinase/Akt signalling and modulation of apoptosis. Although a potent anti-apoptotic effect has been described for RasGAP fragment N (8) and the Akt kinase pathways in general (22,23,39), it is difficult to set the level of RasGAP fragment N detected in NSCLC and SCLC into direct relation with the level of spontaneous and ET-induced apoptosis. There are several important factors that might impair the protective effect of the N-terminal RasGAP fragment and subsequently change the apoptotic phenotype. First, SCLC cell lines express lower levels of RasGAP protein

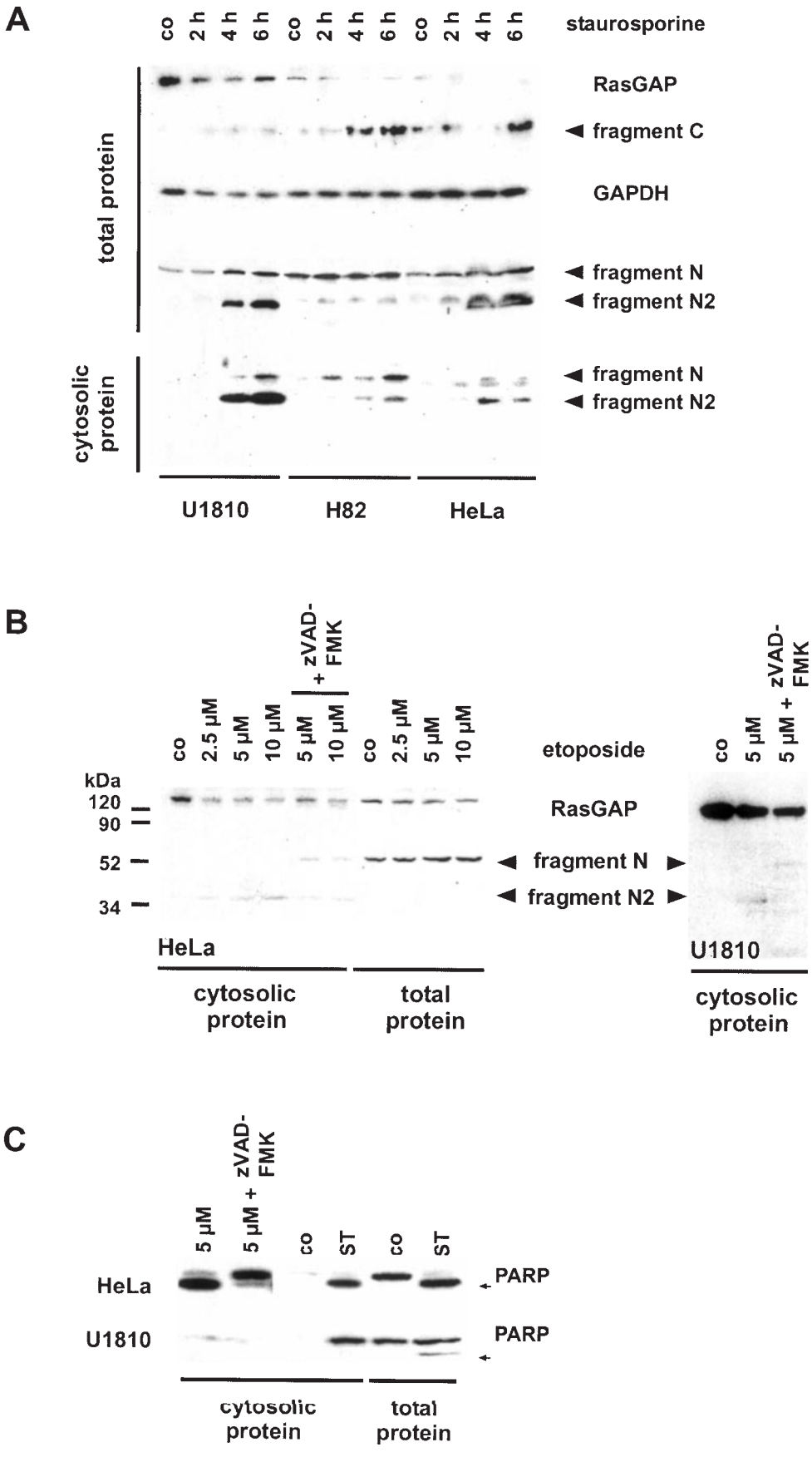

Fig. 7. The indicated cell lines were incubated with ST (1 μM) (**A** and **C**) or ET at the indicated concentrations (ET, 48 h) in the absence or in the presence of zVAD-FMK (20 μM) (**B** and C). The presence of RasGAP and its cleavage fragments (fragments N, N2 and C) (upper two panels), and PARP and its cleavage fragment (bottom panel) were visualized by western blot.

compared with NSCLC. Consequently, the amount of fragment N generated by caspases is reduced despite higher levels of RasGAP processing. Secondly, strong stimulation of caspases in response to chemotherapeutic agents results in the simultaneous formation of RasGAP fragments (N1, N2 and C) that have the ability to potentiate apoptosis (8). This could differentially affect the apoptotic responses in cells that do not activate caspases to the same extent, as observed in NSCLC and SCLC. Thirdly, Akt, the target anti-apoptotic kinase of the RasGAP fragment N pathway, is itself a caspase substrate (43). Consequently an equilibrium between apoptotic and survival signals may rapidly be off-balanced by the negative cross-talks occurring between Akt and the caspases. Fourthly, the caspase-mediated cleavage of RasGAP reduces p120 RasGAP levels and this may weaken the negative regulation of p21 Ras proteins and consequently favour the development of malignant neoplasm (7,29,34). Fifthly, lung cancer cell lines are characterized by several defects in the apoptotic machinery, like the inefficient translocation of key caspases, i.e. active caspase-3, into the nucleus in NSCLC (21) or the defective expression of caspase-8 in SCLC (44). The insensitivity of lung cancer cells to Fas receptor stimulation correlated with the restricted cleavage of RasGAP into fragment N2.

Our findings indicate that spontaneous RasGAP cleavage into fragment N at low caspase activity and the reduced level of p120 RasGAP are associated with higher spontaneous apoptosis in SCLC compared with NSCLC. The anti-apoptotic fragment N might also contribute to the highly malignant and terminally therapy-resistant phenotype of SCLC. In response to ET and induction of higher caspase activity, lung cancer cells stably generate RasGAP fragment N, which does have the potential to impair the complex network of apoptosis. However, compensatory mechanisms triggered by treatment with ET and distinct failures in the apoptotic machinery of lung cancer cells can differently influence the protective effect of the N-terminal RasGAP fragment in NSCLC and SCLC.

Acknowledgements

This work was supported by grants (to B.Z.) from the Swedish (3829-B02-07XBC) and Stockholm (03:173) Cancer Societies, EC-RTD grant (QLK3-CT-2002–01956), by a fellowship for B.B. from the Institute of Environmental Medicine, Karolinska Institutet, and by grants (to C.W.) from the Oncosuisse (OCS 1110-02-2001) and from the Swiss National Science Foundation (3100-066797/1).

References

1. Geenlee,R., Hill-Harmon,M., Murray,T. and Thun,M. (2001) Cancer statistics, 2001. *CA Cancer J. Clin.*, **51**, 15–36.
2. Li,T.K. and Liu,L.F. (2001) Tumor cell death induced by topoisomerase-targeting drugs. *Annu. Rev. Pharmacol. Toxicol.*, **41**, 53–77.
3. Ferraro,C., Quemeneur,L., Fournel,S., Prigent,A.F., Revillard,J.P. and Bonnefoy-Berard,N. (2000) The topoisomerase inhibitors camptothecin and etoposide induce a CD95- independent apoptosis of activated peripheral lymphocytes. *Cell Death Differ.*, **7**, 197–206.
4. Thornberry,N.A. and Lazebnik,Y. (1998) Caspases: enemies within. *Science*, **281**, 1312–1316.
5. Hengartner,M.O. (2000) The biochemistry of apoptosis. *Nature*, **407**, 770–776.
6. Earnshaw,W., Martins,L. and Kaufmann,S. (1999) Mammalian caspases: structure, activation, substrates and functions during apoptosis. *Annu. Rev. Biochem.*, **68**, 383–424.
7. Donovan,S., Shannon,K.M. and Bollag,G. (2002) GTPase activating proteins: critical regulators of intracellular signaling. *Biochim. Biophys. Acta*, **1602**, 23–45.
8. Yang,J.Y. and Widmann,C. (2001) Antiapoptotic signaling generated by caspase-induced cleavage of RasGAP. *Mol. Cell. Biol.*, **21**, 5346–5358.
9. Pomerance,M., Thang,N., Tocque,B. and Pierre,M. (1996) The Ras-GTPase-activating protein SH3 domain is required for Cdc2 activation and mos induction by oncogenic Ras in Xenopus oocytes independently of mitogen-activated protein kinase activation. *Mol. Biol. Cell*, **16**, 3179–3186.
10. Yang,J.Y. and Widmann,C. (2002) The RasGAP N-terminal fragment generated by caspase cleavage protects cells in a Ras/PI3K/Akt-dependent manner that does not rely on NFkappa B activation. *J. Biol. Chem.*, **277**, 14641–14646.
11. Vanhaesebroeck,B. and Alessi,D. (2000) The PI3K-PDK1 connection: more than just a road to PKB. *Biochem. J.*, **346**, 561–576.
12. Datta,S.R., Dudek,H., Tao,X., Masters,S., Fu,H., Gotoh,Y. and Greenberg,M.E. (1997) Akt phosphorylation of BAD couples survival signals to the cell-intrinsic death machinery. *Cell*, **91**, 231–241.
13. Tsuruta,F., Masuyama,N. and Gotoh,Y. (2002) The phosphatidylinositol 3-kinase (PIP3K)-Akt pathway suppresses Bax translocation to mitochondria. *J. Biol. Chem.*, **277**, 14040–14047.
14. Cardone,M.H., Roy,N., Stennicke,H.R., Salvesen,G.S., Franke,T.F., Stanbridge,E., Frisch,S. and Reed,J.C. (1998) Regulation of cell death protease caspase-9 by phosphorylation. *Science*, **282**, 1318–1321.
15. Romashkova,J. and Makarov,S. (1999) NF-kappaB is a target of AKT in anti-apoptotic PDGF signalling. *Nature*, **401**, 86–90.
16. Travis,W., Colby,R., Corrin,B., Shimosato,Y., Brambilla,E., in collaboration with Sobin,L.H. and pathologists from 14 countries (1999) *WHO International Classification of Tumours. Histological Typing of Lung and Pleural Tumours.* Springer, Berlin.
17. Sekido,Y., Fong,K. and Minna,J. (1998) Progress in understanding the molecular pathogenesis of human lung cancer. *Biochim. Biophys. Acta*, **1378**, F21–F59.
18. Comis,R., Friedland,D. and Good,B. (1998) Small-cell lung cancer: a perspective on the past and a preview of the future. *Oncology*, **12**, 44–50.
19. Beck,W.T., Morgan,S.E., Mo,Y.Y. and Bhat,U.G. (1999) Tumor cell resistance to DNA topoisomerase II inhibitors: new developments. *Drug Resist. Updat.*, **2**, 382–389.
20. Joseph,B., Lewensohn,R. and Zhivotovsky,B. (2000) Role of apoptosis in the response of lung carcinomas to anti-cancer treatment. *Ann. N. Y. Acad. Sci.*, **926**, 204–216.
21. Joseph,B., Ekedahl,J., Lewensohn,R., Marchetti,P., Formstecher,P. and Zhivotovsky,B. (2001) Defective caspase-3 relocalization in non-small cell lung carcinoma. *Oncogene*, **20**, 2877–2888.
22. Brognard,J., Clark,A., Ni,Y. and Dennis,P. (2001) Akt/protein kinase B is constitutively active in non-small cell lung cancer cells and promotes cellular survival and resistance to chemotherapy and radiation. *Cancer Res.*, **61**, 3986–3997.
23. Krystal,G., Sulanke,G. and Litz,J. (2002) Inhibition of phosphatidylinositol 3-kinase-Akt signaling blocks growth, promotes apoptosis and enhances sensitivity of small cell lung cancer cells to chemotherapy. *Mol. Cancer Ther.*, **1**, 913–922.
24. Friedman,E. (1995) The role of ras GTPase activating protein in human tumorigenesis. *Pathobiology*, **63**, 348–350.
25. Ekedahl,J., Joseph,B., Grigoriev,M.Y., Muller,M., Magnusson,C., Lewensohn,R. and Zhivotovsky,B. (2002) Expression of inhibitor of apoptosis proteins in small- and non-small-cell lung carcinoma cells. *Exp. Cell Res.*, **279**, 277–290.
26. Joseph,B., Marchetti,P., Formstecher,P., Kroemer,G., Lewensohn,R. and Zhivotovsky,B. (2002) Mitochondrial dysfunction is an essential step for killing of non-small cell lung carcinomas resistant to conventional treatment. *Oncogene*, **21**, 65–77.
27. Susin,S.A., Daugas,E., Ravagnan,L. *et al.* (2000) Two distinct pathways leading to nuclear apoptosis. *J. Exp. Med.*, **192**, 571–580.
28. Heenan,M., Kavanagh,K., Redmond,A., Maher,M., Dolan,E., O'Neill,P., Moriarty,M. and Clynes,M. (1996) Absence of correlation between chemo- and radioresistance in a range of human tumour cell lines. *Cytotechnology*, **19**, 237–242.
29. Iyengar,P. and Tsao,M.-S. (2002) Clinical relevance of molecular markers in lung cancer. *Surg. Oncol.*, **11**, 167–179.
30. Scheffzek,K., Lautwein,A., Scherer,A., Franken,S. and Wittinghofer,A. (1997) Crystallization and preliminary X-ray crystallographic study of the Ras-GTPase-activating domain of human p120GAP. *Proteins*, **27**, 315–318.
31. Davidson,B., Agulansky,L., Goldberg,I., Friedman,E., Ramon,J., Barshack,I. and Kopolovic,J. (1998) Immunhistochemical analysis of rasGTPase activating protein (rasGAP) in prostate cancer. *Pathol. Res. Pract.*, **194**, 399–404.

32. Stahle-Backdhal,M., Inoue,M., Zedenius,J., Sandstedt,B., DeMarco,L., Flam,F., Silfversward,C., Andrade,J. and Friedman,E. (1995) Decreased expression of Ras GTPase activating protein in human trophoblastic tumors. *Am. J. Pathol.*, **146**, 1073–1078.
33. Barshack,I., Goldberg,I., Davidson,B., Ravid,A., Schiby,G., Kopolovic,J., Leviav,A. and Friedman,E. (1998) Expression of rasGTPase activating protein in basal cell carcinoma of the skin. *Mod. Pathol.*, **11**, 271–275.
34. Leblanc,V., Delumeau,I. and Tocque,B. (1999) Ras-GTPase activating protein inhibition specifically induces apoptosis of tumour cells. *Oncogene*, **18**, 4884–4889.
35. Sirzen,F., Zhivotovsky,B., Nilsson,A., Bergh,J. and Lewensohn,R. (1998) Higher spontaneous apoptotic index in small cell compared with non-small cell lung carcinoma cell lines; lack of correlation with Bcl- 2/Bax. *Lung Cancer*, **22**, 1–13.
36. Henkemeyer,M., Rossi,D., Holmyard,D., Puri,M., Mbamalu,G., Harpal,K., Shih,T., Jacks,T. and Pawson,T. (1995) Vascular system defects and neuronal apoptosis in mice lacking ras GTPase-activating protein. *Nature*, **377**, 695–701.
37. Scheffzek,K., Ahmadian,M., Kabsch,W., Wiesmueller,L., Lautwein,A., Schmitz,F. and Wittinghofer,A. (1997) The Ras-RasGAP complex: structural basis for GTPase activation and its loss in oncogenic Ras mutants. *Science*, **277**, 333–338.
38. Leblanc,V., Tocque,B. and Delumeau,I. (1998) Ras-GAP controls Rho-mediated cytoskeletal reorganization through its SH3 domain. *Mol. Cell. Biol.*, **18**, 5567–5578.
39. Kraus,A., Ferber,I., Bachmann,S., Specht,H., Wimmel,A., Gross,M., Schlegel,J., Suske,G. and Schuermann,M. (2002) *In vitro* chemo- and radio-resistance in small cell lung cancer correlates with cell adhesion and constitutive activation of AKT and MAP kinase pathways. *Oncogene*, **21**, 8683–8695.
40. Lee,S., Kim,H., Park,W., Kim,S., Lee,K., Kim,S., Lee,J. and Yoo,N. (2002) Non-small cell lung cancers frequently express phosphorylated Akt; an immunohistochemical study. *Acta Pathol. Microbiol. Immunol. Scand.*, **110**, 587–592.
41. Tang,D., Okada,H., Ruland,J., Liu,L., Stambolic,V., Mak,T. and Ingram,A. (2001) Akt is activated in response to an apoptotic signal. *J. Biol. Chem.*, **276**, 30461–30466.
42. Hill,M., Andjelkovic,M., Brazil,D., Ferrari,S., Fabbro,D. and Hemmings,B. (2001) Insulin-stimulated protein kinase B phosphorylation on Ser-473 is independent of its activity and occurs through a staurosporine-insensitive kinase. *J. Biol. Chem.*, **276**, 25643–25646.
43. Widmann,C., Gibson,S. and Johnson,G. (1998) Caspase-dependent cleavage of signaling proteins during apoptosis. A turn-off mechanism for anti-apoptotic signals. *J. Biol. Chem.*, **273**, 7141–7147.
44. Joseph,B., Ekedahl,J., Sirzen,F., Lewensohn,R. and Zhivotovsky,B. (1999) Differences in expression of pro-caspases in small cell and non-small cell lung carcinoma. *Biochem. Biophys. Res. Commun.*, **262**, 381–387.

Received October 14, 2003; revised December 2, 2003; accepted December 19, 2003